Effort Estimation in Robot-aided Training with a Neural Network

Ana C. de Oliveira, Kevin Warburton, James S. Sulzer, and Ashish D. Deshpande

Abstract— **Robotic exoskeletons open up promising interventions during post-stroke rehabilitation by assisting individuals with sensorimotor impairments to complete therapy tasks. These devices have the ability to provide variable assistance tailored to individual-specific needs and, additionally, can measure several parameters associated with the movement execution. Metrics representative of movement quality are important to guide individualized treatment. While robots can provide data with high resolution, robustness, and consistency, the delineation of the human contribution in the presence of the kinematic guidance introduced by the robotic assistance is a significant challenge. In this paper, we propose a method for assessing voluntary effort from an individual fitted in an upper-body exoskeleton called Harmony. The method separates the active torques generated by the wearer from the effects caused by unmodeled dynamics and passive neuromuscular properties and involuntary forces. Preliminary results show that the effort estimated using the proposed method is consistent with the effort associated with muscle activity and is also sensitive to different levels, indicating that it can reliably evaluate user's contribution to movement. This method has the potential to serve as a high resolution assessment tool to monitor progress of movement quality throughout the treatment and evaluate motor recovery.**

I. Introduction

Annually, 15 million people suffer a stroke around the world [1], and it is the leading cause of long-term disability in the US, leaving a substantial portion of the population with permanent impairments. While traditional clinical interventions [2] have historically seen some recovery of function in the upper-limb, recent robotic interventions have achieved outcomes better or equivalent to conventional therapies with regards to motor function improvement [3], [4], [5].

For robotic therapies to exceed outcomes of conventional therapies, robotic devices must provide 1) biomechanically consistent force application tailored for individual-specific needs and 2) high resolution sensing modalities. In therapeutic interventions for the upper-body, forces applied by robotic devices must be in sync with the natural rhythm of the shoulder girdle [6] to prevent serious shoulder injuries [7], [8]. Despite the promise of robotic rehabilitation and the importance of supporting the shoulder coordination, there has been limited development of interventions that support the coordinated movements in the shoulder complex [9], [10], [11], [12]. The second need for high resolution sensing arises from the shortcomings of the established clinical tests for assessing motor recovery [13]. These tests are often subjective and have a low resolution, which reduces the ability to develop truly individualized interventions. Robots, on the other hand, can provide standardized metrics to assess movement quality with high resolution, robustness, and consistency, and, in some cases, with high correlation with clinical test scores [14].

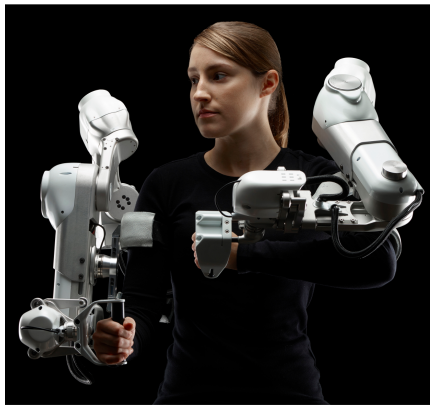

Fig. 1: Harmony, a bimanual upper-body exoskeleton designed to actively control 7 DOF: elevation-depression and protraction-retraction of the shoulder girdle, abduction-adduction, flexion-extension, and medial-lateral rotation of the shoulder, flexion-extension of the elbow.

To address these two needs, we developed the Harmony exoskeleton [15] (Fig. 1). Designed for upper-body rehabilitation, Harmony is a bilateral device that can actively control seven degrees-of-freedom (DOF) on each side of the body, allowing for a wide range of motion (ROM). By actively supporting the shoulder girdle rhythm [16], Harmony supports safe execution of overhead exercises diminishing risks of shoulder impingement and pain. Harmony's capabilities for interaction are complemented by high resolution measurement of position and interaction force, enabling novel, high resolution measurement modalities.

Robotic assessment modality can provide clinicians with high-resolution information that can guide individualized treatment. For this purpose, information must be available for as much of the session as possible. However, during sessions, robots provide kinematic guidance to individuals with moderate to severe motor impairments to change maladaptive behaviors, which affects traditional measures of movement quality based on kinematic metrics, like movement smoothness [17], path length, and hand speed [14], for example. Therefore, in order to evaluate the wearer's movement quality based on kinematic metrics, extra time out of regular sessions is required to capture the kinematic features of the volitional movement under minimal guidance. This reduces the amount of therapy time in a session, potentially reducing efficacy and

This work is supported, in part, by the National Science Foundation, TIRR Foundation, and CAPES (Brazil).

A. C. de Oliveira, K. Warburton, J. S. Sulzer, and A. D. Deshpande (corresponding author) are with the Department of Mechanical Engineering, The University of Texas at Austin, Austin, TX, USA (ana.oliveira, kevinwarburton)@utexas.edu, (james.sulzer, ashish)@austin.utexas.edu

increasing costs of the treatment, and also only provides a limited dataset. Furthermore, the mechanical properties of the robotic device might introduce biases to kinematic metrics, even under minimal or no kinematic guidance [18].

Instead of kinematics, kinetic aspects of movement, such as torques and forces, are available throughout the treatment session, and are therefore a suitable target for developing robotic assessment metrics. One potential approach is using surface electromyography (sEMG) sensors to measure muscle activity. It has been used to measure changes in neuromuscular activity during the training course [19], to measure voluntary effort during completion of different tasks [20], or to quantify abnormal muscle synergies [21]. However, these sensors are cumbersome and time-consuming, rendering them unsuitable to be used in clinical contexts. Other studies use data captured by the robot's sensors in a variety of ways to quantify movement quality and wearer's contributions. It has been proposed that abnormal performance in an end-effector type robot can be quantified using force measurements in the end-effector offset by forces measured during the same motions but with no human volition contribution [22]. This method is limited since it does not allow for any movement or robotic assistance variability, and the motion is limited to a planar surface, which simplifies the dynamic effects of the robot. Another study [23] estimates the joint torques required to move the arm of an individual wearing an exoskeleton-type robot using a dynamic model representing the human arm. By comparing the required forces with the actual forces measured, the wearer's contribution to the movement can be determined. However, individuals with sensorimotor impairments very often exhibit abnormal movement patterns that can be caused by various reasons like exaggerated stretch reflexes, increased muscle tone, and abnormal neural activity [22], and this method cannot differentiate between wearer's volition and involuntary forces caused by abnormal patterns. A Kalman Filter has also been proposed to do sensorless force estimation of the external disturbances in a robotic exoskeleton, which includes the wearer's contributions to the movement, in an implementation of an assist-as-needed strategy that attempts to minimize the amount of guidance provided by the robot [24]. However, this method cannot distinguish between torques caused by unmodeled dynamics from the wearer's volitional efforts.

To address these limitations, we propose a method to assess effort voluntarily generated by individuals fitted with the Harmony exoskeleton. The method consists of estimating the effects of unmodeled dynamics and torques associated with passive and involuntary neuromuscular characteristics using an artificial neural network, which are used to isolate the wearer's voluntary effort. We present preliminary results to validate the method, comparing the estimation with the effort associated with muscle activity recorded using sEMG sensors during elbow flexion-extension. The identification of voluntary effort in individual joints using the proposed method might help unravel joint patterns and maladaptive behaviors in individuals with sensorimotor impairments, and can potentially be used as an assessment tool to monitor progress of movement quality throughout treatment.

II. Materials and methods

A. The Harmony exoskeleton

The Harmony exoskeleton [15] is a bilateral device that can actively control seven DOF in both arms, and has an anatomical shoulder mechanism that can actively support the full mobility of the shoulder. The exoskeleton is attached to the wearer's arm in the middle of the upper-arm and on the hand using a combination of rigid supports and elastic wrapping straps as shown in Fig. 3a. Therefore, the shoulder ball-socket joint, elbow, and forearm are fully assisted, whereas the shoulder girdle is indirectly driven via translation of the glenohumeral joint.

Each of the 14 active DOFs are powered by series elastic actuators (SEA) with dedicated proportional-derivative (PD) torque controllers that allow for implementation of various force and impedance-based therapeutic modes with precise and stable force control [16].

A baseline control ensures dynamic transparency for the user. The system's dynamics is compensated with a feed-forward torque calculated based on the dynamic model of the system implemented using a recursive Newton–Euler method with spatial dynamics representation [25]. Another component of the baseline behavior is an assistance torque to help achieve the proper shoulder coordination. Abnormal coordination within the shoulder is often a symptom observed in stroke victims and movements performed with no regard to this coordination can cause pain, impingement, or injuries to the shoulder. Using a known relation between the angles of the shoulder girdle and the humerus that describes the shoulder coordination in the unaffected population, an impedance controller can be used to induce the correct angles in the shoulder girdle [16].

Other control structures might be added to the baseline control to implement assistive or resistive forces for therapeutic training. The impedance controller represented in (1) was implemented to provide robotic assistance or resistance along a predefined trajectory in joint space.

$$\tau_{task} = K(\theta_{ref} - \theta) + D\dot{\theta} \tag{1}$$

Where K and D are the emulated spring stiffness and damping coefficients.

Even though each actuator can measure torque, the effort applied by the human wearer cannot be distinguished from other unmodeled effects, but it can be estimated as shown in the following subsection.

B. Assessment of voluntary effort

The dynamics of the coupled human-robot system might be represented by the Euler-Lagrange equations of motion (2).

$$M(\theta)\ddot{\theta} + C(\theta,\dot{\theta})\dot{\theta} + F\dot{\theta} + G(\theta) = \tau \tag{2}$$

Torque is measured in each individual joint of the robot, and is a result of a combination of forces generated by

multiple sources, including actuation from the controller τ_u and external forces τ_{ext}.

$$\tau = \tau_u + \tau_{ext}$$

The torque actuation generated by the controller can be broken down into three components, as shown in (3).

$$\tau_u = \tau_{comp} + \tau_{shoulder} + \tau_{task} \tag{3}$$

Where $\tau_{shoulder}$ refers to the torque assistance to help achieve the proper shoulder coordination, τ_{task} represents the torque generated by the impedance controller to drive the robot in a predefined trajectory, and τ_{comp} refers to the torque generated by the dynamics compensation algorithm. Because rehabilitation exercises are usually slow, causing the effect of all other dynamic terms to be insignificant compared to that of gravity [26], and also since the SEA with its torque controller acts like a torque source decoupling the effect of the reflected inertia of the motor rotor [27] further reducing the inertia forces, we herein assume that the inertial, Coriolis, and centrifugal effects are negligible. Therefore

$$\tau_{comp} = \hat{F}\dot{\theta} + \hat{G}(\theta)$$

With $\hat{F}$ and $\hat{G}(\theta)$ representing the friction and gravity matrices, respectively.

Here, we consider that the external torques can be broken down into three components, as shown in (4).

$$\tau_{ext} = \tau_{res} + \tau_{pass} + \tau_{act} \tag{4}$$

where τ_{res} represents the residual torque due to unmodeled dynamics and τ_{act} represents the active torques due to voluntary muscle activity generated by the wearer. The component τ_{pass} reflects the summed effects of passive neuromuscular properties and forces related to involuntary muscle activity [22], mostly caused by exaggerated stretch reflexes and increased muscle tone due to arm mobilization, and abnormal neural activity often observed in individuals with sensorimotor impairments like stroke. Typically, these factors present high inter- and intra-individual variability and depend on many different physical and psychological conditions, making it impossible to model the dynamic behavior of the torque generated by these passive effects.

The external torques can be obtained by subtracting the control actuation τ_u from the measured torque τ. Consider $\tau_e = \tau_{res} + \tau_{pass}$; therefore, τ_{act} can be calculated if τ_e is known.

Passive exercises are a routine part of rehabilitation practice, which can be delivered with robotic assistance. Consider a wearer being passively mobilized along a specific trajectory with robotic assistance, i.e. we assume that $\tau_{act} = 0$; therefore, $\tau_e = \tau_{ext} = \tau - \tau_u$. If the wearer is then asked to voluntarily apply forces along the same trajectory, the kinematic constraints applied in both cases will be similar, such that τ_e will be maintained, but $\tau_{act} \neq 0$.

In order to find τ_{act}, we train an artificial neural network (ANN) (see subsection II-D) to estimate the torques

$$\hat{\tau}_e(\dot{\theta}, \theta) = \hat{\tau}_{res}(\dot{\theta}, \theta) + \hat{\tau}_{pass}(\dot{\theta}, \theta) \tag{5}$$

such that $\hat{\tau}_{act} = \tau_{ext} - \hat{\tau}_e$.

C. Experimental protocol

To validate the proposed method, we designed an experiment consisting of a one DOF movement performed with several levels of active human effort. Muscle activity was measured and used as a ground-truth comparison. The subject was asked to perform elbow flexion and extension while all of the other joints were locked in the configuration shown in Fig. 3a. The desired movement speed was the same across all levels, and was defined by a metronome with auditory and visual feedback indicating directional changes and the desired speed. The movement was repeated ten times in each level.

To control for the level of voluntary effort applied by the wearer, the type of robotic guidance, the impedance controller gains, and the instructions given to the subject were modified to gradually increase the amount of expected voluntary muscle activity, such that the effort would be minimal in the first level and maximal in the last level. Fig. 2 illustrates the levels of expected voluntary effort with the combination of parameters chosen in each level. Level 0 represents the passive mobilization adopted in rehabilitation practice, in which we assume that $\tau_{act} = 0$. Two sets of movements in this level were performed and data from one of these sets was used to train the ANN.

One healthy individual performed the experiment with the right arm only. An sEMG data acquisition system (Delsys Inc., Trigno Wireless EMG) was used to measure muscle activity in the biceps brachii and in the long and lateral heads of triceps brachii. In the analysis, we observed that the lateral head of triceps brachii exhibited patterns that looked like a combination of both the biceps brachii and the long head of triceps brachii activity, which might be caused by sEMG cross-talk due to sensor misplacements. Therefore, the data analysis did not include the lateral head of triceps brachii. Fig. 3 illustrates the experiment setup. The sampling frequency of the sEMG data was 1kHz, and signals were filtered by a fifth-order low-pass Butterworth filter at 5 Hz and normalized to the maximal voluntary contraction (MVC).

Position and torque data from the robot (right arm only) were sampled at 100 Hz and post-processed with a fifth-order moving median filter to remove spikes. Synchronization between the robot data and sEMG data was ensured in the post-process using a spike velocity signal generated by a fast elbow flexion prior to every test.

D. Artificial Neural Network architecture

We used a feed-forward ANN composed of one hidden layer with 15 neurons with the hyperbolic tangent sigmoid transfer function to estimate the function represented in (5), which represents the summed effects of unmodeled dynamics, passive neuromuscular properties and forces associated with involuntary muscle activity. To train the ANN, we used the Levenberg-Marquardt algorithm with the experimental

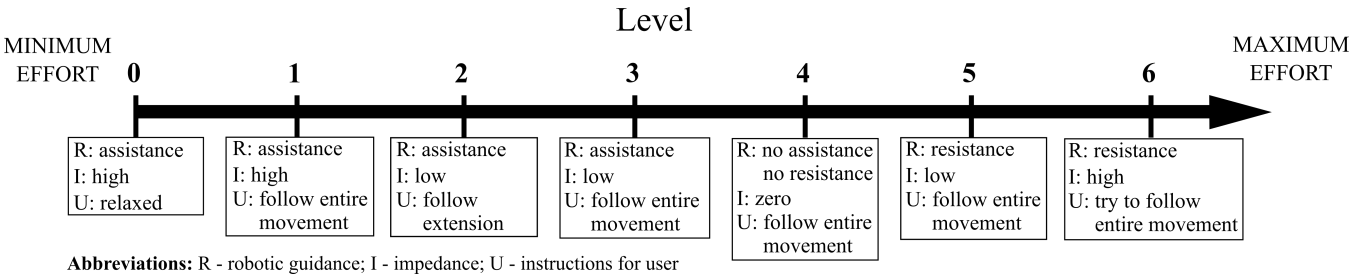

Abbreviations: R - robotic guidance; I - impedance; U - instructions for user

Fig. 2: Levels of expected effort applied by wearer. The combination of parameters in each level is described in the boxes, such that 'R' refers to the type of robotic guidance in the elbow joint (assistance: controller attempts to follow a sinusoidal trajectory given by $\theta(t) = -42sin(2\pi vt)$ where the zero position corresponds to 90° elbow flexion; resistance: controller attempts to hold the joint at the zero position), 'I' refers to the system impedance emulated by the controller in the elbow joint (controller gains for high impedance: $K = 1, D = 0.25$; low impedance: $K = 0.1, D = 0.01$), and 'U' refers to the instructions given to the user.

(a) Subject position. (b) Sensor placement.

Fig. 3: Experiment setup. The subject is attached to the Harmony exoskeleton through the upper-arm and hand, locked in position with just the elbow moving in a flexion-extension motion. sEMG sensors were placed in the biceps and triceps (long and lateral heads) brachii.

data from level 0, where the target output was given by the recorded values of τ_{ext} and the input consisted of the joints positions and velocities vectors stacked together, resulting in a 14-dimensional vector. The ANN output represents the estimate of the 7-dimensional vector $\hat{\tau}_e$.

III. Results

In order to verify consistency of the ANN output, the subject performed two different sets of repetitions in level 0 (no active effort), where we assumed that $\tau_{act} = 0$. One of the collected datasets was used in the ANN training and the other was used for validation. The inputs of the validation dataset were fed to the trained ANN and the generated output was compared with the training target output. The results are shown in Fig. 4. Since the elbow is the only moving joint during the experiments, the inputs and outputs only for the elbow joint are represented.

We used the estimation $\hat{\tau}_e$ to calculate the active torque $\hat{\tau}_{act}$ at a given time. For the elbow joint, positive and negative values of $\hat{\tau}_{act}$ represent extension and flexion torques, respectively. To compare between the estimated active torque and the recorded muscle activity, $\hat{\tau}_{act}$ was normalized with respect to the maximum torque recorded throughout the seven levels of the experiment. Fig. 5 shows the computed values of $\hat{\tau}_e$, $\hat{\tau}_{act}$, and τ_{ext}, as well as a comparison between the normalized $\hat{\tau}_{act}$ and the muscle activity of biceps and triceps brachii normalized to the MVC across the seven levels of the experiment. The correlation coefficients between these parameters for each level was calculated with the Pearson

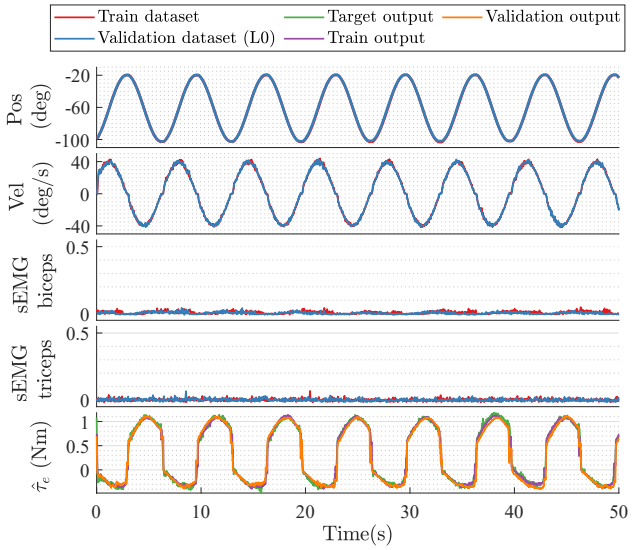

Fig. 4: Validation of the ANN (elbow joint). Time lines are zoomed-in showing only 8 out of ten repetitions performed. sEMG depicted represent values normalized according to the MVC.

correlation, and are shown in Table I. Positive values of $\hat{\tau}_{act}$ were compared with muscle activity in triceps, and negative values were compared with biceps.

TABLE I
CORRELATION COEFFICIENTS
$\hat{\tau}_{act}$ VS. MUSCLE ACTIVITY (NORMALIZED)

Level	Flexion	Extension
L0	-0.03	-0.09
L1	0.74	0.58
L2	0.19	0.61
L3	0.68	0.75
L4	0.30	0.34
L5	0.73	0.83
L6	0.73	0.80

To test the sensibility of the estimated active torque to different levels of voluntary effort, we created a metric called Normalized Integrated Effort (NIE), which can be interpreted as the normalized power exerted within a specific time window, and is calculated using (6), where y represents the effort parameter and t_w represents the time window length.

$$NIE = \frac{\int_0^{t_w} |y| dt}{t_w \times \max(y)} \tag{6}$$

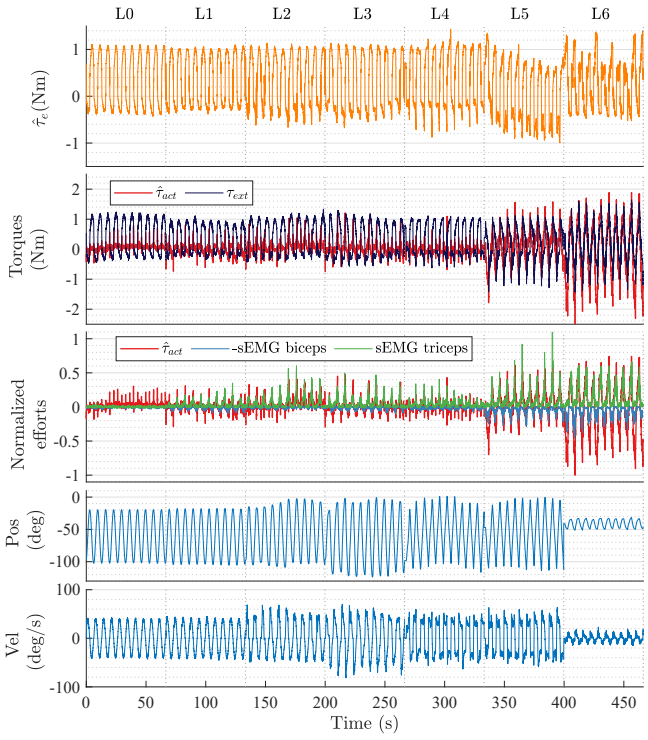

Fig. 5: Results obtained for the elbow joint. Computed values of $\hat{\tau}_e$, $\hat{\tau}_{act}$, and τ_{ext} are presented in the first two rows. Comparison between normalized $\hat{\tau}_{act}$ and muscle activity in flexion and extension for each level is presented in the third row. Negative values of $\hat{\tau}_{act}$ represent flexion torques, and muscle activity in biceps brachii is inverted for comparison purposes only. Recorded positions and velocities are presented in the last two rows.

The NIE varies between 0 and 1, such that 0 represents no effort over the entire time and 1 represents maximal effort over the entire time. Fig. 6 shows the NIE calculated for the seven levels using the biceps and triceps muscle activity, and the estimated active torque split into flexion (negative values) and extension (positive values). The total NIE value is given by the summed quantities of flexion/biceps and extension/triceps.

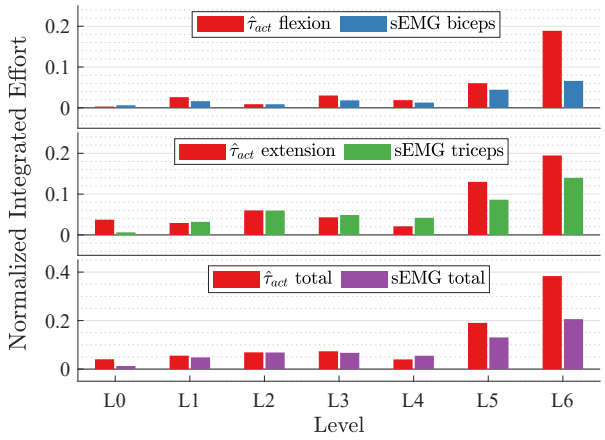

Fig. 6: Normalized integrated effort obtained for each level of the experiment using muscle activity and estimated active torques as parameters. The NIE was calculated separately for flexion and extension, and the total value is given by the summed values.

IV. Discussion

We trained an ANN to estimate $\hat{\tau}_e$ that represents the summed effects of passive neuromuscular properties and forces associated with involuntary muscle activity combined with unmodeled dynamic effects. The assumption that $\tau_{act} = 0$ in level 0 was confirmed by the muscle activity recorded shown in Fig. 4, where small variations in the biceps activity can be attributed to motion artefacts due to relative movement between the electrode and muscle. The output generated for the validation input data consistently tracked the target output, as shown in Fig. 4.

To obtain the active torque $\hat{\tau}_{act}$ representing the voluntary effort we used the estimation $\hat{\tau}_e$ combined with τ_{ext}. Because of the simplicity of the motion performed, one may argue that $\hat{\tau}_{act}$ and τ_{ext} are likely to exhibit a high correlation. In Fig. 5, the comparison between the active and external torques shows that this is in fact true in levels 5 and 6, when the active torques applied by the wearer are much larger than torques generated by residual dynamics and passive and involuntary characteristics. However, this correlation decreases as the active torque applied is reduced, as shown in Fig. 5, emphasizing the need for the proposed method to identify a wide range of effort levels.

It is not expected that the estimated active torque will track the measured muscle activity, because muscle moment-arms vary with joint angle, causing the relationship between muscle contraction and joint torque to be nonlinear [28]. However, it is still expected that they will be correlated, and the coefficients shown in Table I indicate high correlations for all levels but levels 0 and flexion phase of level 2. In Fig. 5 we can observe that, $\hat{\tau}_{act}$ exhibits multiple peaks in level 0, which are likely the cause for the observed low correlation coefficient. These peaks could be due to multiple reasons. First, it might be related with noise produced by the ANN when the velocity is close to zero, which is likely to happen in all levels, but it is more noticeable in level 0. Another possible cause is the residual inertial effects not compensated in the robot's baseline control. These effects are negligible when the movement velocity is low, but they become significant during directional shifts. Because acceleration was not used as an input parameter, these effects might not be captured by the ANN estimation of $\hat{\tau}_e$. Therefore, they are encapsulated in $\hat{\tau}_{act}$, and in cases where the active effort is negligible, like in level 0 and flexion phase of level 2, the difference with respect to muscle activity will become more pronounced.

A metric called NIE was introduced to verify the reliability and sensibility of $\hat{\tau}_{act}$ to different levels of voluntary effort. The experiment performed was designed such that the total voluntary effort required is expected to monotonically increase from level 0 to level 6. This increase in partially confirmed by the NIE calculated with muscle activity, depicted in Fig. 6, but there is an unexpected decrease in level 4, both in flexion and extension phases. This might be caused by a difference in effort input associated with variations in movement speed between the robotic assistance

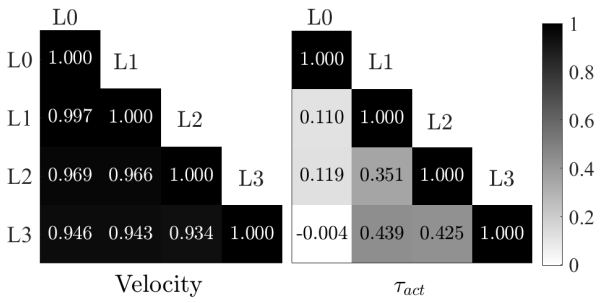

Fig. 7: Pearson correlation between different levels for velocity and active torque curves.

and human volitional motion. Movement speed executed by the robot during assisted movements is constant over time, and if the robot moves in a speed slightly lower than the human voluntary motion, the robot will apply a resistive force and the wearer will exert a higher effort to follow the trajectory. When assistance is removed, which is the case in level 4, the wearer will apply less effort to complete the movement, but will most likely exhibit a different velocity profile. This effect can be observed in Fig. 5, where the amplitude of the muscle activity of both biceps and triceps decreases overall in level 4 compared with level 3, and the velocity profile changes significantly. Nevertheless, the NIE values calculated with the estimated active torque still closely matches the values calculated with muscle activity. We can observe an increasing difference between the NIEs in levels 5 and 6. This might be related with significant differences in position and velocity profiles in levels 4, 5, and particularly in level 6, when compared with the other levels, as shown in Fig. 5. Furthermore, inertia effects might be encapsulated in the estimation, and these two factors together likely contribute to a biased estimation of $\hat{\tau}_{act}$, which explains the observed differences in the NIE values.

In order to verify the differences in sensitivity of velocity and active torque to different human contributions to the assisted movement, we calculated pair-wise Pearson correlations for the velocity and active torque between the levels for all possible combinations. Note that we only included the levels where the robot was assisting the wearer to complete the motion, which consists of levels zero through three, as detailed in Fig. 2. These correlations are depicted in Fig. 7. The depicted correlations for velocity curves are close to one in all cases, whereas the correlations for active torque are lower than 0.5 in all cases. This emphasizes that kinematic measures such as velocity are not suitable to represent human contributions to assisted movements. On the other hand, the results presented suggest that $\hat{\tau}_{act}$ has the potential to represent human effort in individual joints during robot-aided training, because it produces results consistent with effort associated with muscle activity and it is also sensitive to different levels of effort.

The proposed method can be further expanded to include other joints in analysis of complex multi-joint movements. Even though the estimated torques might not be directly associated with anatomical joints because not all the links of Harmony are rigidly attached to the human arm, the estimation can still indicate torque patterns and couplings that can be useful in the analysis of movement quality of individuals with sensorimotor impairments.

V. Conclusion

In this paper, we proposed a method for assessment of voluntary effort applied by the wearer using the Harmony exoskeleton. An ANN was used to estimate the torques generated by unmodeled robot dynamics and by the summed effects of passive neuromuscular properties and involuntary forces, which were used to calculate the active torque applied by the human. The estimation was consistent with the efforts associated with muscle activity, and it reliably tracked variable levels of effort.

Limitations of this study include the restricted range of kinematic conditions of the training data and the lack of acceleration data to estimate $\hat{\tau}_e$. The training data was captured in a single kinematic condition, and estimation for movements that exhibit large deviations from this condition, either in position or velocity profiles, will most likely have significant biases. Further development and testing is needed to examine the suitability of this method when the movement being assessed is practiced with no robotic assistance. In future works we plan to record training data in a broad spectrum of conditions with different velocity profiles to allow a wider range of movement variations. Although this might represent an overhead time when applying the method as an assessment tool for rehabilitation, the process to capture training data consists of a passive mobilization intervention, which is already a routine practice used to optimize joint position and to regain soft tissue length, and might bring extra benefits to the wearer associated with wider joint ROM [29]. Regarding the lack of acceleration data in the estimation of $\hat{\tau}_e$, this limits the ability of the ANN to include residual inertial effects in the estimation, especially when the position and velocity profiles of the input data differ from the training profiles. Consequently these effects get encapsulated in the active torque, and is particularly concerning when no or little effort is being applied. Acceleration was not included in this study because reliable measurements are not available in our case so far. Modifications in the ANN can be made to attempt to overcome this issue, and will be explored in future studies.

The proposed experiment has little chance of confounding factors due to its simplicity, and the results show that the proposed method has great potential to provide a good estimation of voluntary effort generated by a person wearing the Harmony exoskeleton. This estimation can potentially capture human contributions to the movement that are not perceived via kinematic metrics. Also, the method might be expanded to include other joints in analysis of complex multi-joint movements, where the estimated effort might be used to unravel joint patterns and compensations in individuals with sensorimotor impairments, and can potentially serve as a high resolution assessment metric to monitor progress of movement quality throughout the treatment.

REFERENCES

[1] J. Mackay and G. A. Mensah, *The atlas of heart disease and stroke*. World Health Organization, 2004.

[2] C. J. Winstein, J. Stein, R. Arena, B. Bates, L. R. Cherney, S. C. Cramer *et al.*, "Guidelines for Adult Stroke Rehabilitation and Recovery," *Stroke*, vol. 47, no. 6, pp. e98–e169, jun 2016.

[3] J. Mehrholz, T. Platz, J. Kugler, and M. Pohl, "Electromechanical and Robot-Assisted Arm Training for Improving Arm Function and Activities of Daily Living After Stroke," *Stroke*, vol. 40, no. 5, pp. e392–e393, 2009.

[4] G. Kwakkel, B. Kollen, and H. Krebs, "Effects of robot-assisted therapy on upper limb recovery after stroke: a systematic review," *Neurorehabilitation and neural Repair*, 2007.

[5] B. R. Brewer, S. K. McDowell, and L. C. Worthen-Chaudhari, "Post-stroke Upper Extremity Rehabilitation: A Review of Robotic Systems and Clinical Results," *Topics in Stroke Rehabilitation*, vol. 14, no. 6, pp. 22–44, dec 2007.

[6] V. T. Inman, L. C. Abbott *et al.*, "Observations on the function of the shoulder joint," *JBJS*, vol. 26, no. 1, pp. 1–30, 1944.

[7] T. Najenson, E. Yacubovich, and S. S. Pikielni, "Rotator cuff injury in shoulder joints of hemiplegic patients." *Scandinavian journal of rehabilitation medicine*, vol. 3, no. 3, pp. 131–137, 1971.

[8] P. E. Kaplan, J. Meridith, G. Taft, and H. B. Betts, "Stroke and brachial plexus injury: a difficult problem." *Archives of physical medicine and rehabilitation*, vol. 58, no. 9, pp. 415–418, 1977.

[9] T. Nef, M. Guidali, and R. Riener, "ARMin III - arm therapy exoskeleton with an ergonomic shoulder actuation," *Applied Bionics and Biomechanics*, vol. 6, no. 2, pp. 127–142, jul 2009.

[10] H. S. Park, Y. Ren, and L. Q. Zhang, "IntelliArm: An exoskeleton for diagnosis and treatment of patients with neurological impairments," *Proceedings of the 2nd Biennial IEEE/RAS-EMBS International Conference on Biomedical Robotics and Biomechatronics, BioRob 2008*, pp. 109–114, 2008.

[11] S. J. Ball, I. E. Brown, and S. H. Scott, "MEDARM: A rehabilitation robot with 5DOF at the shoulder complex," *IEEE/ASME International Conference on Advanced Intelligent Mechatronics, AIM*, no. April 2017, 2007.

[12] A. Zeiaee, R. Soltani-Zarrin, R. Langari, and R. Tafreshi, "Design and kinematic analysis of a novel upper limb exoskeleton for rehabilitation of stroke patients," in *2017 International Conference on Rehabilitation Robotics (ICORR)*. IEEE, 2017, pp. 759–764.

[13] L. Santisteban, M. Térémetz, J.-P. Bleton, J.-C. Baron, M. A. Maier, and P. G. Lindberg, "Upper Limb Outcome Measures Used in Stroke Rehabilitation Studies: A Systematic Literature Review," *Plos One*, vol. 11, no. 5, p. e0154792, 2016.

[14] S. M. Mostafavi, P. Mousavi, S. P. Dukelow, and S. H. Scott, "Robot-based assessment of motor and proprioceptive function identifies biomarkers for prediction of functional independence measures," *Journal of NeuroEngineering and Rehabilitation*, vol. 12, no. 1, pp. 1–12, 2015.

[15] B. Kim and A. D. Deshpande, "An upper-body rehabilitation exoskeleton Harmony with an anatomical shoulder mechanism: Design, modeling, control, and performance evaluation," *The International Journal of Robotics Research*, vol. 36, no. 4, pp. 414–435, 2017.

[16] ——, "Controls for the shoulder mechanism of an upper-body exoskeleton for promoting scapulohumeral rhythm," in *2015 IEEE International Conference on Rehabilitation Robotics (ICORR)*. IEEE, 2015, pp. 538–542.

[17] S. Balasubramanian, A. Melendez-Calderon, A. Roby-Brami, and E. Burdet, "On the analysis of movement smoothness," *Journal of NeuroEngineering and Rehabilitation*, vol. 12, no. 1, p. 112, dec 2015.

[18] C. G. Rose, E. Pezent, C. K. Kann, A. D. Deshpande, and M. K. O'Malley, "Assessing Wrist Movement With Robotic Devices," *IEEE Transactions on Neural Systems and Rehabilitation Engineering*, vol. 26, no. 8, pp. 1585–1595, 2018.

[19] X. L. Hu, K. Y. Tong, R. Song, X. J. Zheng, K. H. Lui, W. W. Leung *et al.*, "Quantitative evaluation of motor functional recovery process in chronic stroke patients during robot-assisted wrist training," *Journal of Electromyography and Kinesiology*, vol. 19, no. 4, pp. 639–650, 2009.

[20] G. N. Lewis and E. J. Perreault, "An assessment of robot-assisted bimanual movements on upper limb motor coordination following stroke," *IEEE Transactions on Neural Systems and Rehabilitation Engineering*, vol. 17, no. 6, pp. 595–604, 2009.

[21] P. C. Kung, C. C. K. Lin, and M. S. Ju, "Neuro-rehabilitation robot-assisted assessments of synergy patterns of forearm, elbow and shoulder joints in chronic stroke patients," *Clinical Biomechanics*, vol. 25, no. 7, pp. 647–654, 2010.

[22] P. S. Lum, C. G. Burgar, D. E. Kenney, and H. F. Van Machiel Der Loos, "Quantification of force abnormalities during passive and active-assisted upper-limb reaching movements in post-stroke hemiparesis," *IEEE Transactions on Biomedical Engineering*, vol. 46, no. 6, pp. 652–662, 1999.

[23] H. A. Abdullah, C. Tarry, R. Datta, G. S. Mittal, and M. Abderrahim, "Dynamic biomechanical model for assessing and monitoring robot-assisted upper-limb therapy," *The Journal of Rehabilitation Research and Development*, vol. 44, no. 1, p. 43, 2007.

[24] A. U. Pehlivan, D. P. Losey, and M. K. Omalley, "Minimal Assist-as-Needed Controller for Upper Limb Robotic Rehabilitation," *IEEE Transactions on Robotics*, vol. 32, no. 1, pp. 113–124, 2016.

[25] R. Featherstone and D. Orin, "Robot Dynamics : Equations and Algorithms Foundational Work in Robot Dy," *Tensor*, vol. 1, no. April, pp. 826–834, 2000.

[26] J. M. Hollerbach and T. Flash, "Dynamic interactions between limb segments during planar arm movement," *Biological cybernetics*, vol. 44, no. 1, pp. 67–77, 1982.

[27] H. Vallery, J. Veneman, E. Van Asseldonk, R. Ekkelenkamp, M. Buss, and H. Van Der Kooij, "Compliant actuation of rehabilitation robots," *IEEE Robotics & Automation Magazine*, vol. 15, no. 3, pp. 60–69, 2008.

[28] G. J. Ettema, G. Styles, and V. Kippers, "The moment arms of 23 muscle segments of the upper limb with varying elbow and forearm positions: Implications for motor control," *Human Movement Science*, vol. 17, no. 2, pp. 201–220, 1998.

[29] J.-M. Gracies, "Pathophysiology of impairment in patients with spasticity and use of stretch as a treatment of spastic hypertonia," *Physical medicine and rehabilitation clinics of North America*, vol. 12, no. 4, pp. 747–768, 2001.